Supplementary Information for

Late-Eocene to early Oligocene productivity events in the proto-southern Ocean as drivers of global cooling and Antarctica glaciation

Gabrielle R. de Faria[1,2], David Lazarus[1], Johan Renaudie, Jessica[1] Stammeier[3], Volkan Özen[1,2], Ulrich Struck[1,2]

[1] Museum für Naturkunde, Leibniz Institute for Evolution and Biodiversity Science, Invalidenstraße 43, 10115, Berlin, Germany

[2] Freie Universität Berlin, Institute for Geological Sciences, Malteserstraße 74-100, 12249 Berlin, Germany

[3] GFZ German Research Centre for Geosciences, Telegrafenberg, 14473 Potsdam, Germany

Contents of this file

Introduction

This supplement includes the age models for ODP sites 1090, 748, 689 (Figures S1 to S3), as well as for ODP Site 738 (Figure S4) as we compare our results to published data from this site, and the age model(s) are relevant to our interpretations. It also includes sedimentation rates compared to biogenic barium accumulation rates (Figure S5). Tables S1 and S2 show the data included in our compilation of Neodymium isotopes and atmospheric carbon dioxide.

Figures S1 to S4:
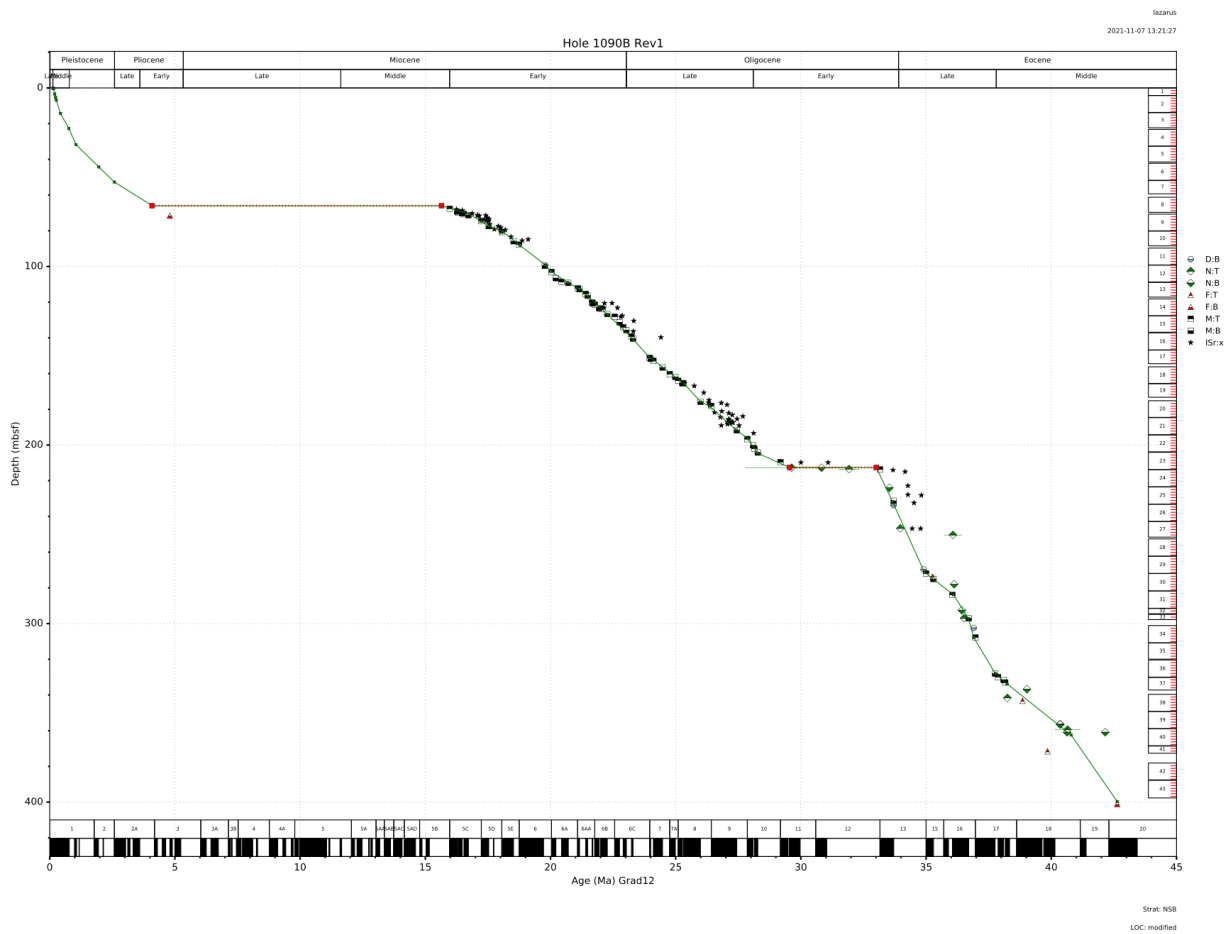
Figure S1. Age depth plot, ODP Site 1090. This site benefits from a robust paleomagnetic stratigraphy supported by coherent multiple fossil group biostratigraphy, and in the late Eocene - Oligocene strontium isotope stratigraphy. Sources of geochronologic data and interpretations are given in detail in Channell et al. (2003). D - diatom, F - planktonic foraminifera, I - isotope (Strontium, Oxygen event, etc.), M - paleomagnetic stratigraphy reversal boundary pick, N - calcareous nannofossil, R - radiolaria; B - bottom, T - top. Other plotting conventions for these and other age depth plots in this SOM are given in the description of the plotting program ADP (Renaudie et al., 2020) and the companion user guide to the program (https://github.com/plannapus/nsb_adp_wx/releases). All age models, and the data used to create them, are available at the NSB website (https://nsb.mfn-berlin.de)

689B rev3, Paleogene events checked for correct evaluation and entry

Site 689D rev1 dbl 24.9.20
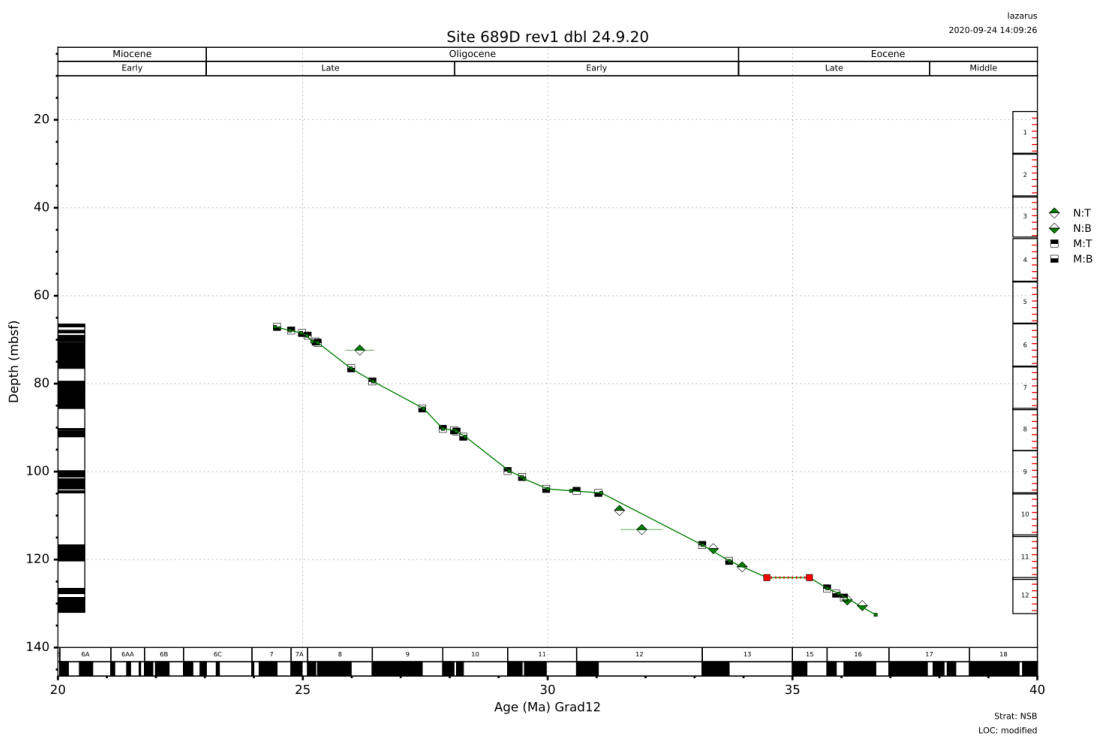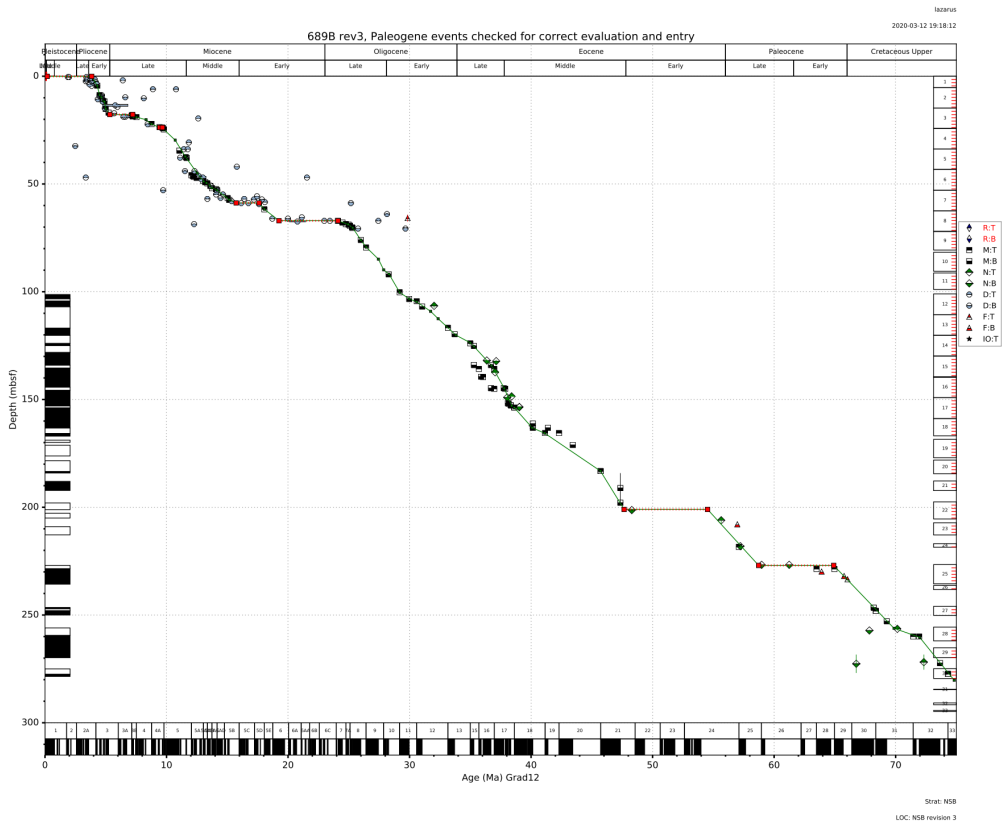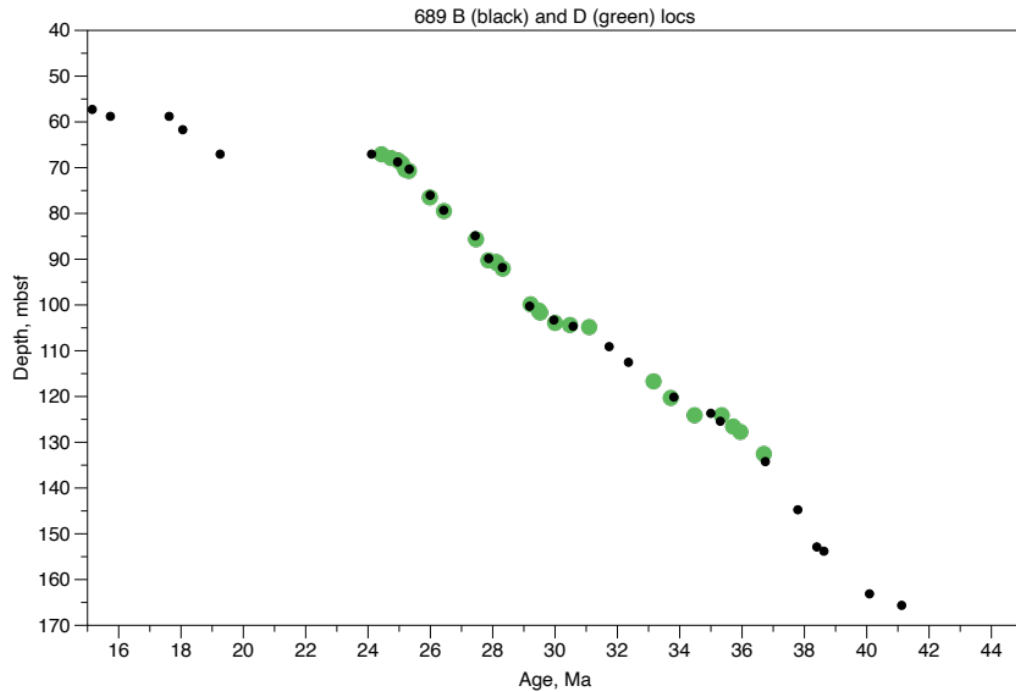
Figure S2 a-c Southern Ocean, Maud Rise ODP Site 689, holes B (top) and D (bottom) age-depth plots, and a cross-plot showing coherency between holes. This site has had multiple rounds of stratigraphic study and revision. The original paleomagnetic stratigraphy interpretation of Spiess (Leg volume Science Report) for Hole B was re-evaluated and questionable magnetic data removed from the polarity interpretation (shown along the depth axis on left). Polarity intervals based on single samples were removed, and intervals of more than a couple meters with no measurements were shown as no data rather than as a continuous polarity interval. Florindo et al. (2005) created new data for Hole D and cross-compared the holes at selected intervals. This evaluation was used and extended to other depth intervals here, and as a result some polarity reversal boundaries were re-assigned to a different GPTS boundary. Both the older and new picks are shown on the plot for Hole 689B. As noted by Florindo et al.(2005) paleomagnetic stratigraphy at this site becomes unreliable below about 38 Ma.
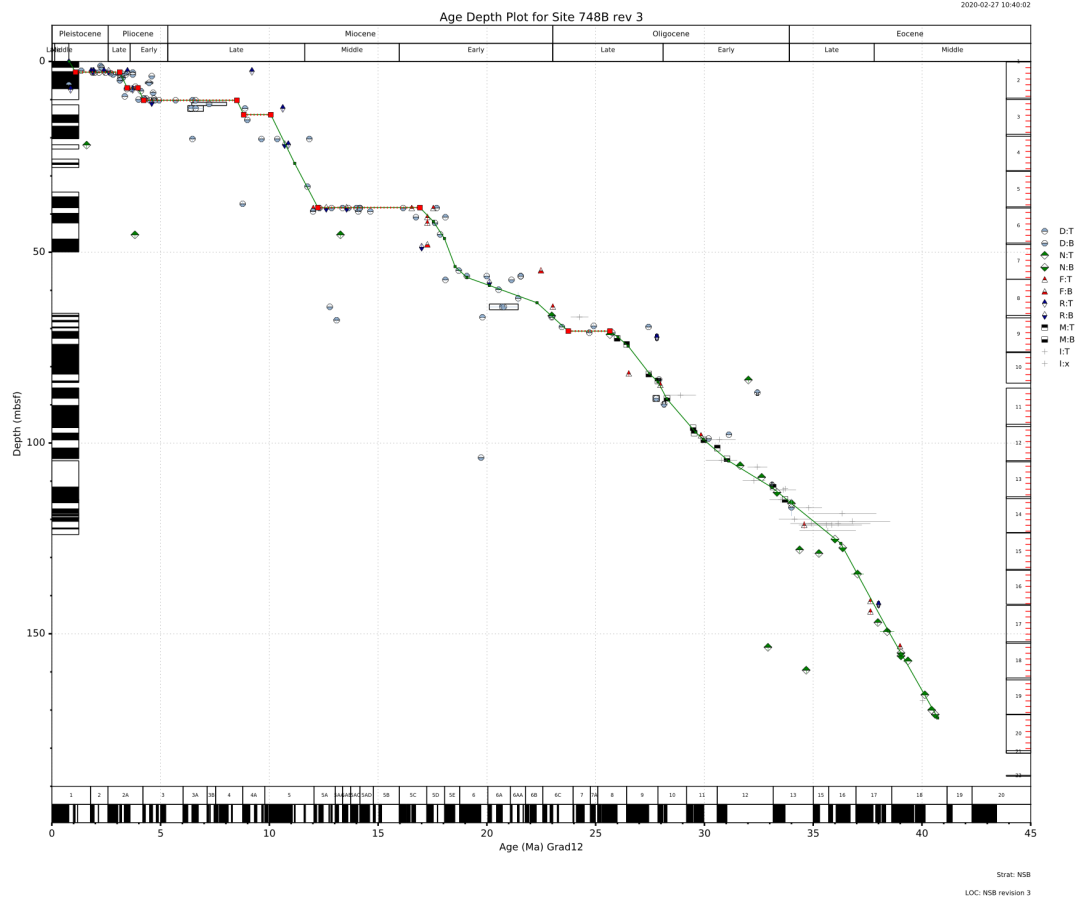
Figure S3: Southern Ocean, Kerguelen Plateau, ODP Site 748, hole B, age-depth plot. The Paleogene part of this Site was restudied, diatom events were recalibrated, strontium isotope data were generated and a new paleomagnetic stratigraphy was developed by Roberts et al (2003). Their interpretation is followed here. The Neogene has not yet been similarly revised.

a)
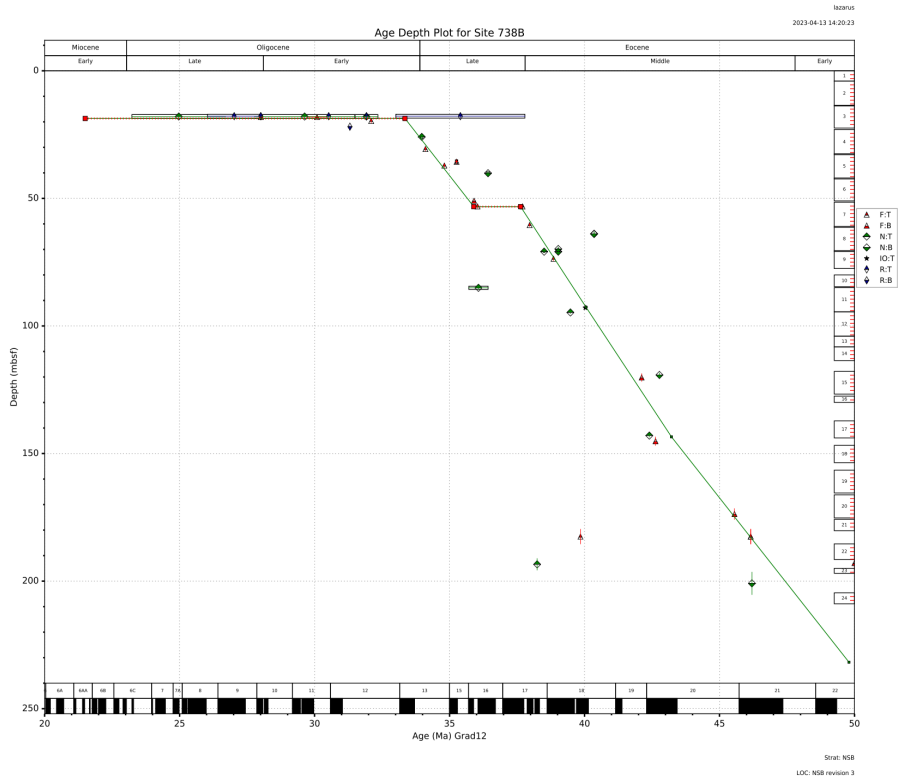
b)
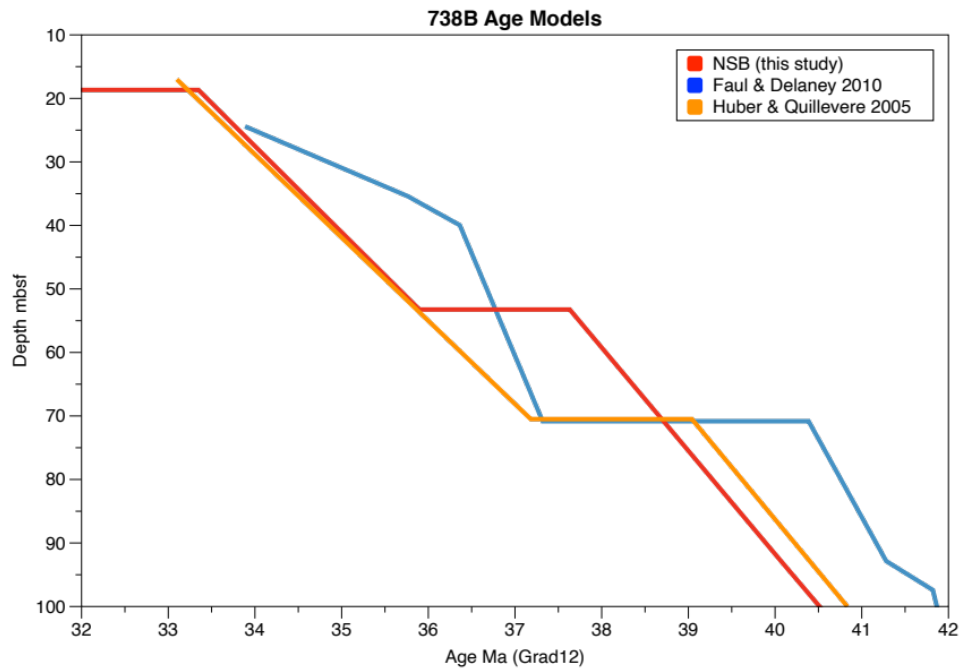
Figure S4a-b: Southern Ocean, Kerguelen Plateau, ODP Site 738, hole B, age-depth plot, and alternative age models from the recent literature. Although there have been several studies and revisions of chronostratigraphic information for the older Paleogene part of this site (below ca 40 Ma) the late Eocene interval remains problematic and different interpretations are possible. Here we show, in addition to that used in our study, those of Huber and Quillevere (2005) and Faul and Delaney (2010). Differences in ages and sedimentation rates are substantial and thus productivity proxies based on accumulation rate are uncertain for the late Eocene interval of this site.
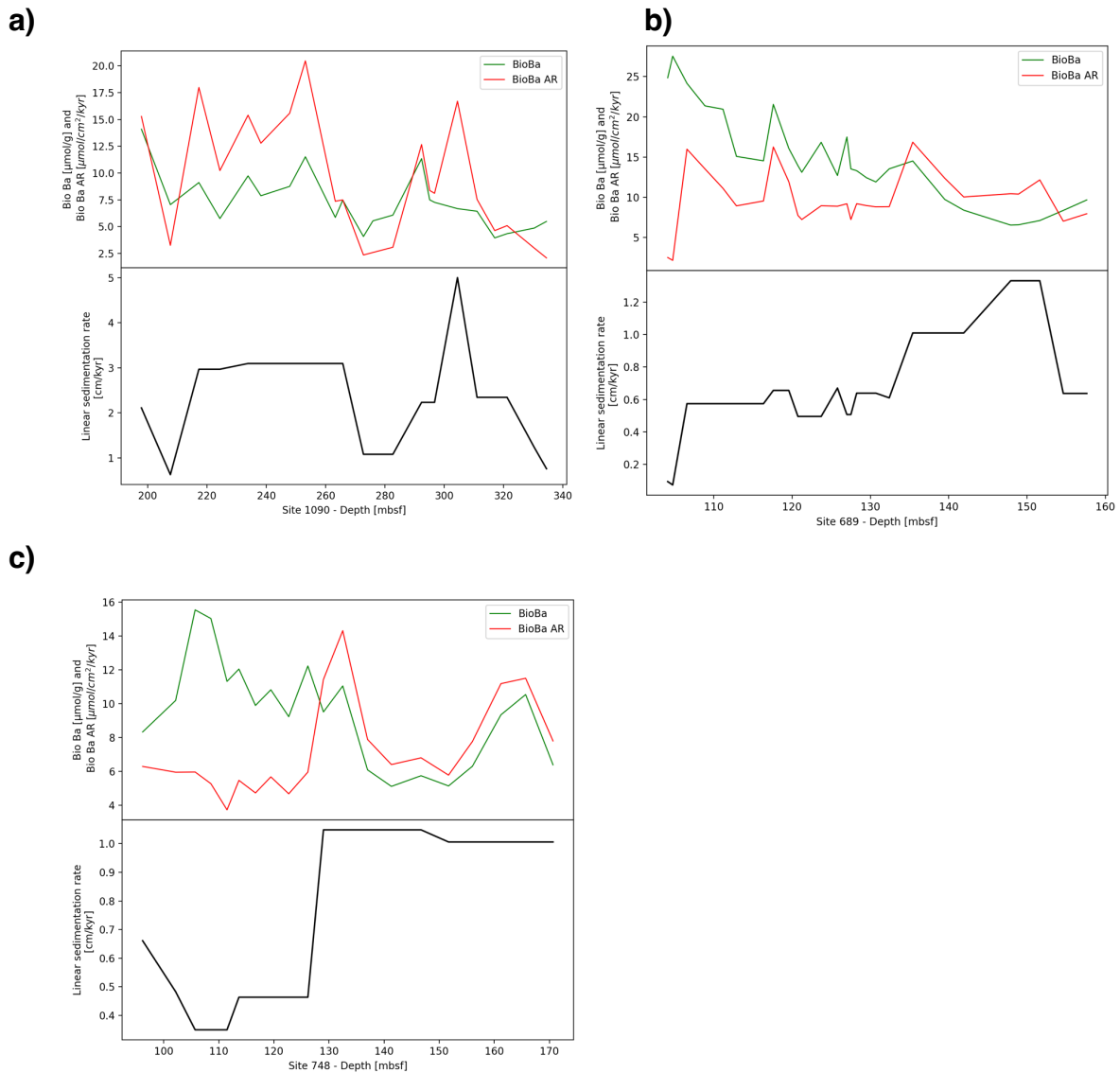
Figure S5: Biogenic barium accumulation rates, Bio Ba AR and sedimentation rate ODP Site 1090(a), ODP Site 689 (b), ODP Site 748 (c).
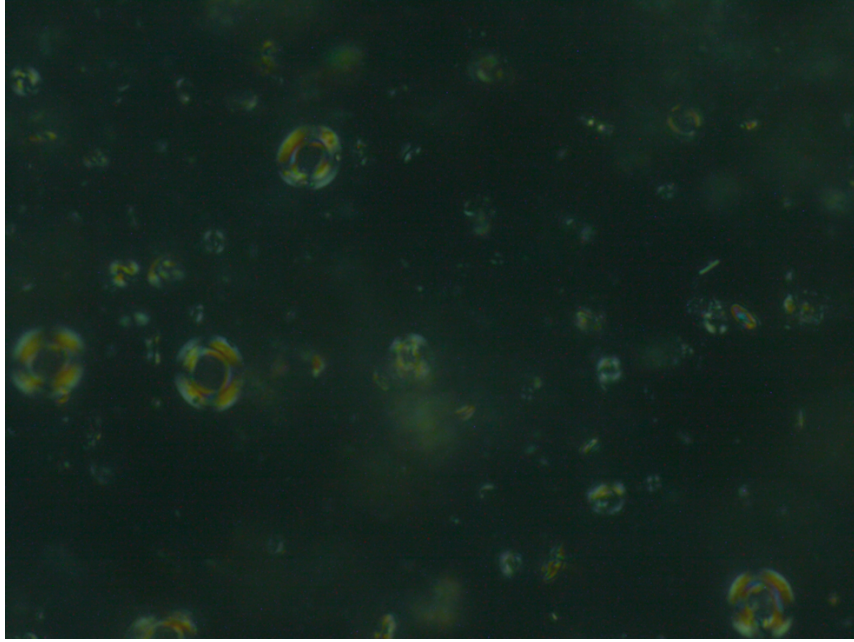
Figure S6: Polarised Microscope image from fine fraction sediments (<45µm) - coccoliths.
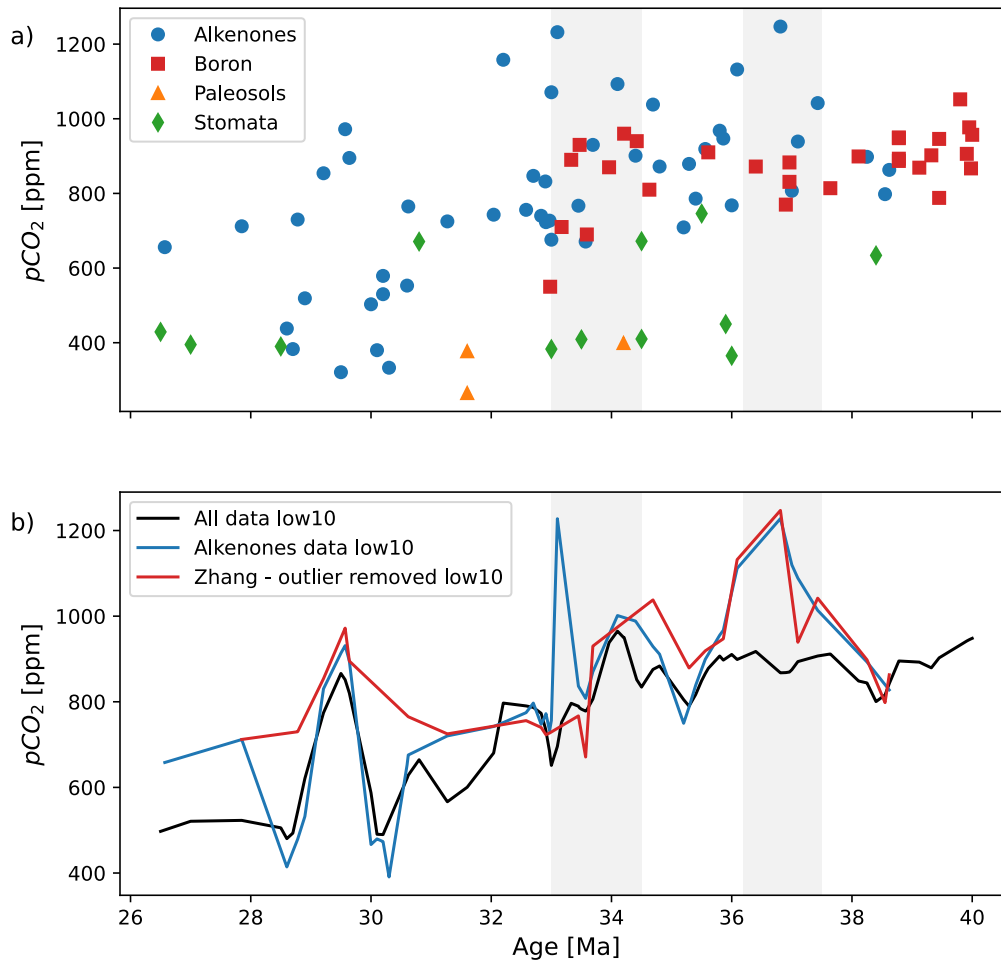
Figure S7: Compilation of paleo atmospheric pCO2 reconstructions. a) data from marine and terrestrial archives.b) Lowess fitted smoothed curves to various compilations of proxy pCO2 data: Black - all proxy data, including also Boron, paleosol and stomata estimates. Blue - all data from a single proxy (alkenones). Red - Single site alkenone proxy data from Zhang, with single outlier (>> 2,000 ppm) removed - same time series as in main text Figure 4.

Data sources given in Table S2. Other than a single outlier point (all alkenone curve, ca 33.1 Ma), Alkenone curves show coherent pattern of maximum values near 37 Ma, followed by declining values until ca 35 Ma, a smaller peak at ca 34.5, and a rapid decline at ca 34 Ma. Data younger than ca 32 Ma is relatively sparse and different data subsets do not show the same degree of coherency, although all agree on eventual decline to values near 40 ppm by ca 25 Ma.

Table S1: Neodymium isotopes data compilation from fossil fish teeth from the locations investigated in this study.

Sites	Hole	Location	Reference
1090	B	Agulhas Ridge, South Atlantic Ocean	Scher and Martin [2006]
689	B	Maud Rise, Southern Ocean	Scher and Martin [2004]
738	B	Kerguelen Plateau, Indian Ocean	Scher and Delaney [2010]
738	B	Kerguelen Plateau, Indian Ocean	Scher et al. [2011]
738	B	Kerguelen Plateau, Indian Ocean	Scher et al. [2014]
748	B	Kerguelen Plateau, Indian Ocean	Wright et al. [2018]
744	A	Kerguelen Plateau, Indian Ocean	Wright et al. [2018]

Table S2: pCO2 data compilation

Reference	Method	Sites	Location
Pagani et al. 2005 (and 1999a, 1999b updated by Henderiks and Pagani 2008).	Alkenones	DSDP[b] Sites 511, 513, 516 and 612 ODP Site 803	Atlantic Ocean Equatorial Pacific
Zhang et al. [2013]	Alkenones	ODP[a] Site 925 A	Western equatorial Atlantic Ocean
Anagnostou et al. [2016]	Boron isotopes	TDP 12 e 13	Tanzania
Anagnostou et al. [2020]	Boron isotopes	ODP Site 865	Equatorial Pacific
Henehan et al. [2020]	Boron Isotopes	ODP Site 1260 ODP Site 865	Equatorial Atlantic Equatorial Pacific
Pearson et al. [2009] (updated by Anagnostou et al. 2016)	Boron isotopes	TDP[c] 12 e 13	Tanzania
Breecker and Retallack, [2014]	Paleosols		
Ekart et al. [1999]	Paleosols		
Kohn et al. [2015]	Paleosols		
Srivastava et al. [2013]	Paleosols		
Doria et al. [2011]	Stomata		
Erdei et al. [2012]	Stomata		
Grein et al. [2013] (updates Roth-Nebelsick et al.2004, 2012)	Stomata		
Kürschner et al. [2008]	Stomata		
Reichgelt et al. [2016]	Stomata		
Retallack [2009]	Stomata		
Roth-Nebelsick et al. [2012]	Stomata		
Roth-Nebelsick et al. [2014]	Stomata		
Steinthorsdottir et al. [2016]	Stomata		
Sun et al. [2017]	Stomata		

Note: [a] Ocean Drilling Program; [b] Deep Sea Drilling Project; [c]Tanzanian Drilling Project